

Short Communication

## Low Temperature Synthesis of $\alpha$ -LiFeO<sub>2</sub> Nanoparticles and Its Behavior as Cathode Materials for Li-ion Batteries

Yanmei Ma<sup>1</sup>, Yongchun Zhu<sup>1,\*</sup>, Yang Yu<sup>1</sup>, Tao Mei<sup>1</sup>, Zheng Xing<sup>1</sup>, Xing Zhang<sup>1</sup> and Yitai Qian<sup>1,2,\*</sup>

<sup>1</sup> Hefei National Laboratory for Physical Science at Microscale and Department of Chemistry, University of Science and Technology of China, Hefei, Anhui 230026, PR China

<sup>2</sup> School of Chemistry and Chemical Engineering, Shandong University, Jinan 250100, PR China

\*E-mail: [ytqian@ustc.edu.cn](mailto:ytqian@ustc.edu.cn); [yhzhu@ustc.edu.cn](mailto:yhzhu@ustc.edu.cn)

Received: 21 March 2012 / Accepted: 2 April 2012 / Published: 1 May 2012

---

$\alpha$ -LiFeO<sub>2</sub> nanoparticles with the size of ~10 nm were synthesized at 120 °C by a molten salt route. As controlling the molar ratios of starting materials, crystallized  $\alpha$ -LiFeO<sub>2</sub> or Fe<sub>2</sub>O<sub>3</sub> nanoparticles with similar size can be selectively produced.  $\alpha$ -LiFeO<sub>2</sub> nanoparticles were applied as cathode material for Li-ion batteries (LIBs), which showed an initial discharge capacity of 138 mAh/g, together with a capacity of 91 mAh/g after 300 cycles (66% capacity retention) at 1.0 C. Moreover, they presented an initial discharge capacity of 71 mAh/g, retaining 62 mAh/g after 300 cycles (87% capacity retention) even at 2.0 C.

---

**Keywords:**  $\alpha$ -LiFeO<sub>2</sub>; nanoparticles; discharge capacity; Lithium-ion batteries

### 1. INTRODUCTION

Owing to its relative more economical, environmental benignity and better safety during operation, LiFeO<sub>2</sub> has important advantages as cathodic materials for LIBs compared with LiCoO<sub>2</sub> and LiNiO<sub>2</sub> [1,2,3]. LiFeO<sub>2</sub> have various crystalline structures, such as the cubic disordered rocksalt-type  $\alpha$  phase,  $\beta$ -layer [4],  $\gamma$ -layer (structure similar to  $\alpha$ -NaFeO<sub>2</sub>) [5,6,7], corrugated layer (structure similar to  $\gamma$ -FeOOH) [5,8], goethite-type (structure similar to  $\alpha$ -FeOOH) [9], hollandite-type LiFeO<sub>2</sub> (structure similar to  $\beta$ -FeOOH) [8], and non-stoichiometric compounds with mixed structures [10,11,12]. Among these phases,  $\alpha$  [13], corrugated [13], goethite-type [13] and hollandite-type [14,15] LiFeO<sub>2</sub> had been manifested to be electrochemical active so far [16].

For  $\alpha$ -LiFeO<sub>2</sub> phase, Li<sup>+</sup> and Fe<sup>3+</sup> randomly occupy the octahedral sites [17].  $\alpha$ -LiFeO<sub>2</sub> was synthesized through the method of ionic exchange reactions in molten salts from  $\alpha$ -NaFeO<sub>2</sub> for the first time [5]. And then other methods had been used to prepare  $\alpha$ -LiFeO<sub>2</sub>. For instance,  $\alpha$ -LiFeO<sub>2</sub>

nanoparticles with the size of ~50 nm was prepared by solid state reaction at 250 °C, which presented a capacity of 150 mAh/g at 0.25 C in the range of 4.5-1.5 V after 50 cycles [18]. Large-scale  $\alpha$ -LiFeO<sub>2</sub> nanorods were synthesized via a molten salt synthesis method at 250 °C, which showed a capacity of 80 mAh/g at a current density of 0.1 mA/cm<sup>2</sup> (2.0-4.2 V) [19].  $\alpha$ -LiFeO<sub>2</sub> nanoparticles with sizes of ~10 to 20 nm were also prepared by a molten salt reaction at 120 °C and followed by annealing at 300 °C. when they were used as cathodic materials for LIBs, the as-obtained products showed an initial discharge capacity of 284 mAh/g, and the capacity dropped rapidly after 30 cycles, and after 100 cycles, the discharge capacity was measured to be 120 mAh/g, which was around 42% of the initial discharge capacity at 0.5 C [20].

In this study,  $\alpha$ -LiFeO<sub>2</sub> nanoparticles with the size of ~10 nm had been prepared by one step molten salt route at 120 °C. The as-obtained nanoparticles showed initial capacities of 138 and 71 mAh/g at 1.0 and 2.0 C. Even after 300 cycles, the capacities remained 91 and 62 mAh/g, capacity retention were 66% and 87%, respectively.

## 2. EXPERIMENTAL

### 2.1. Synthesis

All reagents were analytical grade and were purchased from Shanghai Chemical Industrial Corp, and used without further purification. In a typical procedure, 100 mmol LiOH·H<sub>2</sub>O, 100 mmol LiNO<sub>3</sub> and FeCl<sub>3</sub>·6H<sub>2</sub>O with different amounts were mixed and grinded in different agate mortar to obtain homogenous compositions, here amount of FeCl<sub>3</sub>·6H<sub>2</sub>O were 5 mmol, 10 mmol and 20 mmol, respectively. Then 50 ml H<sub>2</sub>O<sub>2</sub> (30%) were added into the each mixture dropwise and stirred for 3 h with medium speed. Then the mixtures were heated at 120 °C in the different beakers for 4 h in a oven, and they were cooled down to room temperature. The resulting products were washed by deionized water and ethanol for several times, then centrifuged and dried in a vacuum oven at 60 °C for 12 h.

### 2.2. Chemical characterization

The phase identification of the products were accomplished using powder X-ray diffraction (XRD), employing a Philips X'pert X-ray diffractometer with Cu K $\alpha$  radiation ( $\lambda = 1.54178 \text{ \AA}$ ). A scan rate of 0.05 deg/s was applied to record the pattern in the  $2\theta$  range of 20~85°. The particles morphology and microstructure were observed on a high-resolution transmission electron microscope (HRTEM, JEOL-2010) with an accelerating voltage of 200 kV and the selected area electron diffraction (SAED).

### 2.3. Electrochemical characterizations

$\alpha$ -LiFeO<sub>2</sub> had been studied as cathode material for LIBs. Here the electrochemical behaviors of  $\alpha$ -LiFeO<sub>2</sub> nanoparticles were measured via CR 2016 coin-type cells, in which lithium

metal foil was used as the counter electrode. Test cells were assembled in a dry argon-filled glove box. The test cell consisted of a working electrode and lithium sheet which was separated by a Celgard 2300 membrane and electrolyte of 1 M LiPF<sub>6</sub> in EC–EMC (1 : 1v/v) in volume. Then the  $\alpha$ -LiFeO<sub>2</sub> nanoparticles, acetylene black, and polyvinylidenedifluoride (PVDF) were homogeneously mixed in a weight ratio of 75:15:10 in an acid washed agate mortar. The working electrode consisted of 75 wt% active material. Finally, Such the electrode sheets were dried in a vacuum oven at 100 °C for 12 h before electrochemical evaluation, and then charge-discharge tests were performed in the potential range of 1.5-4.5 V (Li<sup>+</sup>/Li) at 1.0 C and 2.0 C on a LAND2001A automatic battery tester (Wuhan China) at room temperature.

### 3. RESULTS AND DISCUSSION

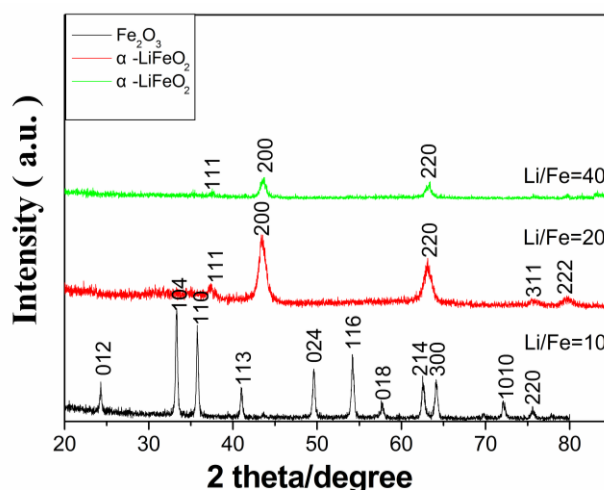


**Figure 1.** XRD patterns of the as-obtained products ( $\alpha$ -LiFeO<sub>2</sub> and Fe<sub>2</sub>O<sub>3</sub>)

Fig. 1 shows the XRD pattern of the product obtained when the amount of raw material FeCl<sub>3</sub>·6H<sub>2</sub>O was 5 mmol (Li/Fe = 40) or 10 mmol (Li/Fe = 20). All the diffraction peaks can be clearly indexed as rocksalt-type  $\alpha$ -LiFeO<sub>2</sub> consistent with JCPDS File No. 74-2284 with space group of Fm3m. Fig. 2a, b exhibits the TEM images of the as-obtained  $\alpha$ -LiFeO<sub>2</sub>. From the HRTEM image of nanoparticles (Fig. 2b), the crystallite size was clearly observed as ~10 nm. The HRTEM image of the polycrystalline  $\alpha$ -LiFeO<sub>2</sub> is shown in Fig. 2c. The measured lattice spacing of 0.233 nm is in good agreement with the d-spacing of the (111) of the  $\alpha$ -LiFeO<sub>2</sub>. Fig. 2d shows the corresponding SAED pattern of the as-obtained  $\alpha$ -LiFeO<sub>2</sub> products, here all of the ring spots were evaluated to represent d-spacings of 0.233, 0.20, 0.14, 0.125 and 0.12 nm, which could be referred to the crystallographic directions of (111), (200), (220), (311) and (222), respectively.

In this case, the molar ratio of Li/Fe exerts a significant influence on the final products.  $\alpha$ -LiFeO<sub>2</sub> is the main product as the molar ratio of the source materials to Li/Fe = 20. Increasing the ratio to Li/Fe = 40, the products are still  $\alpha$ -LiFeO<sub>2</sub>. On the contrary,  $\alpha$ -LiFeO<sub>2</sub> could not be obtained and Fe<sub>2</sub>O<sub>3</sub> was obtained instead when the molar ratio of Li/Fe was decreased to Li/Fe = 10. XRD pattern

shown in Fig. 1. All the diffraction peaks can be clearly indexed as  $\text{Fe}_2\text{O}_3$  consistent with JCPDS File No. 84-0307.

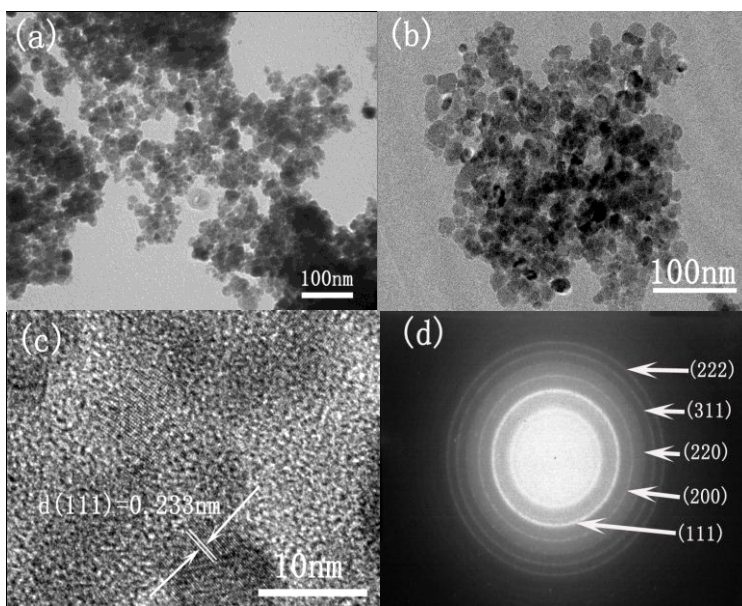


**Figure 2.** (a) TEM image of as-obtained  $\alpha\text{-LiFeO}_2$  nanoparticles; (b) and (c) HRTEM images; (d) SAED patterns of the as-obtained  $\alpha\text{-LiFeO}_2$  nanoparticles.

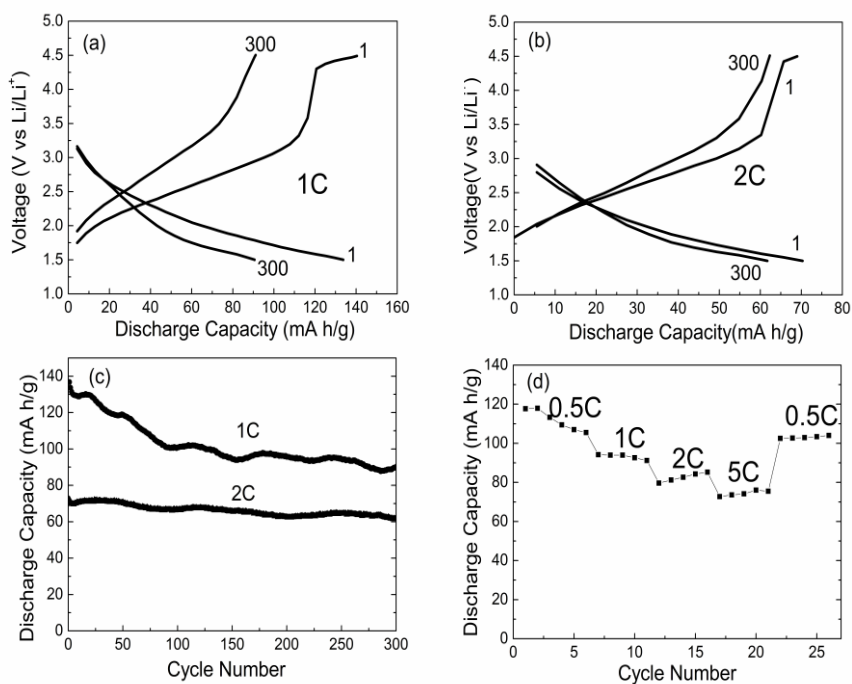


**Figure 3.** (a) The charge-discharge curves of the  $\alpha\text{-LiFeO}_2$  nanoparticles at the 1 and 300 cycles at 1.0 C; (b) The charge-discharge curves of the  $\alpha\text{-LiFeO}_2$  nanoparticles at the 1 and 300 cycles at 2.0 C; (c) discharge capacity curve vs cycle number for nanoparticles at 1.0 C and 2.0 C; (d) discharge capacity curve vs cycle number of nanoparticles at the different rates.

The electrochemical performances of the as-prepared  $\alpha$ -LiFeO<sub>2</sub> nanoparticles were evaluated as cathode materials for LIBs. Fig. 3a, b show the typical charge-discharge curves for the first and 300th cycles of  $\alpha$ -LiFeO<sub>2</sub> at 1.0 and 2.0 C between 1.5 and 4.5 V. It can be clearly seen that there is electrochemical plateau in the 1.9-2.2 V region at both rates. The cycling stabilities of  $\alpha$ -LiFeO<sub>2</sub> nanoparticle electrodes at 1.0 C and 2.0 C are shown in Fig. 3c. It is noted that the discharge capacity has a weak decay step by step at 1.0 C, nevertheless the discharge capacity is still up to 91 mAh/g even after 300 cycles, which is around 66% of the initial discharge capacity. When the rate is raised to 2.0 C, the discharge capacity is measured to be 62 mAh/g after 300 cycles at 2.0 C, which is around 87% of the initial discharge capacity. The cycling performance of the  $\alpha$ -LiFeO<sub>2</sub> nanoparticle electrodes at different charge-discharge rates were measured after 5 cycles at each rate from 0.5 C to 5.0 C in an ascending order, followed by a return to 0.5 C, is shown in Fig. 3d. The discharge capacities are measured as 109, 94, 83, 74 and 103 mAh/g at the rates of 0.5, 1.0, 2.0, 5.0 and 0.5 C, respectively. When the rate is decreased to 0.5 C after 20 cycles, the reversible capacity of the  $\alpha$ -LiFeO<sub>2</sub> is still 103 mAh/g.

It is found that the cycling stability of the  $\alpha$ -LiFeO<sub>2</sub> electrode at 2.0 C is better than that at 1.0 C, and this phenomenon was also observed in LiMnO<sub>2</sub> [21] and LiMn<sub>2</sub>O<sub>4</sub> [22] materials. The nanoparticles with smaller size could facilitate the contact between active materials and electrolyte and shorten lithium path [23,24], which may be favorable for the improvement of their electrochemical performance.

#### 4. CONCLUSIONS

$\alpha$ -LiFeO<sub>2</sub> nanoparticles with the size of ~10 nm were synthesized at 120 °C by one step molten salt route. As they applied as cathode material for LIBs. Electrochemical measurements showed that the first run discharge capacities of the  $\alpha$ -LiFeO<sub>2</sub> nanoparticles were 138 and 71 mAh/g at 1.0 C and 2.0 C, and remained 91 and 62 mAh/g after 300 cycles, respectively.

#### ACKNOWLEDGEMENTS

This work was financially supported by the National Natural Science Fund of China (No. 91022033), the 973 Project of China (No. 2011CB935901)

#### References

1. Y. Yu, L. Gu, C.L. Wang, A. Dhanabalan, P.A. Van Aken, J. Maier, *Angew. Chem Int. Ed*, 48 (2009) 6485–6489
2. A.L.M. Reddy, M. Shaijumon, S.R. Gowda, P.M. Ajayan, *Nano Lett*, 9 (2009) 1002–1006
3. M. S. Park, G. X. Wang, Y. M. Kang, D. Wexler, S. X. Dou, H. K.Liu, *Angew. Chem. Int. Ed*, 46 (2007) 750
4. M. Tabuchi, S. Tsutsui, C.Masquelier, R. Kanno, K. Ado, I.Matsubara, S.Nasu, H. Kageyama, *J. Solid State Chem*, 140 (1998) 159

5. T. Shirane, R. Kanno, Y. Kawamoto, Y. Takeda, M. Takano, T. Kamiyama, F. Izumi, *Solid State Ionics*, 79 (1995) 227
6. M. Tabuchi, C. Masquelier, et al, *Solid State Ionics*, 90 (1996) 129
7. R. Kanno, T. Shirane, Y. Inaba, Y. Kawamoto, *J. Power Sources*, 68 (1997) 145
8. T. Matsumura, R. Kanno, Y. Inaba, Y. Kawamoto, M. Takano, *J. Electrochem. Soc.*, 149 (2002) A1509–A1513
9. Y. Sakurai, H. Arai, S. Okada, J.-I. Yamaki, *J. Power Sources*, 68 (1997) 711
10. J. Kim, A. Manthiram, *J. Electrochem Soc.*, 146 (1999) 4371
11. Z. Han, X. Chen, W. Zhang, C. Zhong, H. Zhao, Y. Qian, *Mater. Chem. Phys.*, 69 (2001) 292
12. S.H. Wu, H.Y. Liu, *Journal of Power Sources*, 174 (2007) 789–794
13. Y. Sakurai, H. Arai, J. Yamaki. *Solid State Ionics*, 113–115 (1998) 29–34
14. A. Robert Armstrong, Daniel W. Tee, Fabio La Mantia, Petr Novak and Peter G. Bruce, *J. AM. CHEM. SOC.*, 130 (2008) 3554-3559
15. T. Matsumura, R. Kanno, Y. Inaba, et al, *Journal of Electrochemistry Society*, 149 (2002) A1509
16. Jiangang Li, Jianjun Li, Jing Luo, Li Wang, Xiangming He, *Int. J. Electrochem. Sci*, 6 (2011)
17. M. Barré, M. Catti, *J. Solid State Chem*, 182 (2009) 2549–2554
18. J. Morales, J. Santos-Pen, *Electrochemistry Communications*, 9 (2007) 2116–2120
19. X. Wang et al. *Journal of Crystal Growth*, 265 (2004) 220–223
20. Md. Mokhlesur Rahman, Jia-Zhao Wang, Mohd Faiz Hassan, Shulei Chou, Zhixin Chenc and Hua Kun Liua, *Energy Environ. Sci*, 4 (2011) 952–957
21. E. Hosono et al, *Journal of Power Sources*, 195 (2010) 7098–7101
22. Kuthanapillil M. Shaju and Peter G. Bruce, *Chem. Mater*, 20 (2008) 17
23. S. Y. Zeng, K. B. Tang, T.W. Li, Z. H. Liang, D.Wang, Y. X. Qi and W. W. Zhou, *J. Phys. Chem. C*, 112 (2008) 4836–4843
24. L. Croguennec, P. Deniard, and R. Brec, *J. Electrochem. Soc.*, 144 (1997) 3323